

1 **Oral feeding with probiotic *Lactobacillus rhamnosus* attenuates cigarette smoke-induced COPD in**

2 **C57Bl/6 mice: Relevance to inflammatory markers in human bronchial epithelial cells**

3

4 **J.L. Carvalho¹, M. Miranda¹, A.K. Fialho¹, H. Castro-Faria-Neto², E. Anatriello¹, A.C. Keller³, F.**

5 **Aimbire¹**

6

7 ¹Department of Science and Technology, Federal University of São Paulo, São José dos Campos, SP,

8 Brazil; ²Laboratory of Immunopharmacology, FioCruz, Rio de Janeiro, Brazil;

9 ³Department of Microbiology, Immunology and Parasitology, Federal University of São Paulo, São

10 Paulo, SP, Brazil

11

12

13

14 **Corresponding author:**

15 flavio.aimbire@unifesp.br

16

17 **Short title:** *Lactobacillus rhamnosus* attenuates *in vivo* COPD

18 Abstract

19 COPD is a prevalent lung disease with significant impacts on public health. Affected airways
20 exhibit pulmonary neutrophilia and consequent secretion of pro-inflammatory cytokines and proteases,
21 which result in lung emphysema. Probiotics act as nonspecific modulators of the innate immune system
22 that improve several inflammatory responses. To investigate the effect of *Lactobacillus rhamnosus* (*Lr*) on
23 cigarette smoke (CS)-induced COPD C57Bl/6 mice were treated with *Lr* during the week before COPD
24 induction and three times/week until euthanasia. For *in vitro* assays, murine bronchial epithelial cells as
25 well as human bronchial epithelial cells exposed to cigarette smoke extract during 24 hours were treated
26 with *Lr* 1 hour before CSE addition. *Lr* treatment attenuated the inflammatory response both in the airways
27 and lung parenchyma, reducing neutrophilic infiltration and the production of pro-inflammatory cytokines
28 and chemokines. Also, *Lr*-treated mice presented with lower metalloproteases in lung tissue and lung
29 remodeling. In parallel to the reduction in the expression of TLR2, TLR4, TLR9, STAT3, and NF- κ B in
30 lung tissue, *Lr* increased the levels of IL-10 as well as SOCS3 and TIMP1/2, indicating the induction of an
31 anti-inflammatory environment. Similarly, murine bronchial epithelial cells as well as human bronchial
32 epithelial cells (BEAS) exposed to CSE produced pro-inflammatory cytokines and chemokines, which
33 were inhibited by *Lr* treatment in association with the production of anti-inflammatory molecules.
34 Moreover, the presence of *Lr* also modulated the expression of COPD-associated transcription found into
35 BALF of COPD mice group, i.e., *Lr* downregulated expression of NF- κ B and STAT3, and inversely
36 upregulated increased expression of SOCS3. Thus, our findings indicate that *Lr* modulates the balance
37 between pro- and anti-inflammatory cytokines in human bronchial epithelial cells upon CS exposure and it
38 can be a useful tool to improve the lung inflammatory response associated with COPD.

39
40 **Keywords:** COPD; lung inflammation; airway remodeling; toll-like receptor; transcription factors; human
41 bronchial epithelial cell; probiotic

43 **1. Introduction**

44 Although chronic obstructive pulmonary disease (COPD) is one of the major chronic health
45 conditions in which disability and death rates are increasing worldwide, the development of new strategies
46 to disease management remains underwhelming [1-3]. Although the intrinsic factors that contribute to
47 COPD development remains subject of discussion, the cigarette smoke is well recognized as a risk factor for
48 the disease [3].

49 Chemokines such as CXCL1 and CXCL8 as well as cytokines TNF, IL-1 β , IL-6, and IL-17 are
50 chemotactic factors that attract inflammatory cells to the injured lung, principally neutrophils and
51 monocyte-derived macrophage [4-7], where the pulmonary destruction initiates, compromising the alveolar
52 parenchyma [8]. Exacerbated activity of metalloproteinases from neutrophils in COPD patients is
53 responsible for destruction of alveolar parenchyma [9-12]. In COPD, neutrophils release proteinases into
54 lung milieu, such as metalloproteases MMP-9 and MMP-12, result in emphysema [13] where the immune
55 system switches to a Th17 response to promote the perpetuation of inflammation [14]. The effects of
56 matrix metalloproteinase (MMP) can be inhibited by tissue inhibitors of metalloproteinase (TIMP) secreted
57 by several cells [15]. During the pathogenesis of COPD, the balance between the effects of MMP and its
58 TIMP is dysregulated [16-18], since that MMP released by neutrophils overlaps with TIMP activity with
59 consequent pulmonary tissue destruction.

60 In parallel to the cytokine storm, the transcription factors NF- κ B and the balance between STAT3/SOCS3
61 (suppressor of cytokine signaling 3) signaling are also present in the COPD pathogenesis through secretion
62 of pro-inflammatory mediators, such as TNF, IL-8, IL-33, CXCL1, CXCL9, and CCL2 from bronchial
63 epithelial cells [19, 20]. Some authors have evidenced an unbalanced SOCS3/STAT3 in *in vivo* COPD as
64 well as in emphysematous patients [21-23]. This phenomenon is characterized by a reduced SOCS3
65 expression associated with increased STAT3 causing pulmonary fibrosis.

66 Cigarette pollutants can directly trigger pathogen-associated molecular patterns (PAMPs) such as toll-like
67 receptors (TLRs), particularly TLR2 and TLR4, to initiate pattern recognition [24]. TLRs are present in
68 dendritic cells, alveolar macrophages, neutrophils, and epithelial cells, and they have been correlated to
69 lung inflammation caused by COPD [3]. Among them, the expression of TLR2, TLR4, and TLR9 is
70 elevated in monocytes and TLRs are associated with number of sputum neutrophils, secretion of pro-

71 inflammatory cytokines, and lung function impairment [25-27]. This is a reflex of the immune dysfunction
72 observed in COPD [28, 29].
73 Some airways structural cells, such as the bronchial epithelium, when exposed to cigarette smoke secrete
74 pro-inflammatory mediators activating alveolar macrophages as well as attracting neutrophils and activated
75 lymphocytes towards the injured tissue [13, 30]. In fact, the airway epithelial cells are interface between
76 innate and adaptive immunity. Moreover, the bronchial epithelial cells also discharge transforming growth
77 factor- β (TGF β), which triggers fibroblast proliferation for tissue remodeling [14, 31]. Therefore, small
78 airway-wall remodeling strongly contributes to airflow limitation in COPD, decline in lung function, and
79 poor responses to available therapies [32-34].
80 Due to the high morbidity and the limitations of existing COPD treatments [1, 35], innovative action is
81 needed against airway inflammation as well as lung emphysema to better control the disease. One effective
82 treatment for COPD may be to attenuate immune response driven to pro-inflammatory mediators and at the
83 same time upregulate the secretion of anti-inflammatory proteins in lung milieu. Therefore, the ability of
84 probiotics to modulate the immune response and the effects of their use to prevent the development of
85 various chronic diseases, including COPD and asthma, has caught the attention of many researchers [36-
86 40]. Little is known, however, concerning the nature of the probiotic-host cell interactions, or how these
87 interactions could be manipulated to obtain stronger regulatory responses in treatment against COPD.
88 Thus, we aim to investigate whether the oral feeding with probiotic *Lactobacillus rhamnosus* can
89 beneficially modulate the immune response and attenuate lung inflammatory response in *in vivo* COPD
90 model induced by cigarette smoke.

91

92 **2. Material and Methods**

93 **2.1. Animals**

94 Three-month-old male C57Bl/6 mice were used. They were purchased from Center for the
95 Development of Experimental Models (CEDEME) of the Federal University of São Paulo (UNIFESP),
96 housed under controlled humidity, light and temperature conditions, inside ventilated polyethylene cages,
97 in the vivarium located at Science and Technology Institute at the UNIFESP in São José dos Campos, SP,
98 Brazil. The animals had food (Nuvilab – Quimtia, Brazil) and water ad libitum. The mice were

99 anesthetized with ketamine (100 mg/kg) and xylazine (10 mg/kg) via i.p. and euthanized with excess
100 anesthetics. The experiments were approved according to CONCEA (2016) and the Research Ethics
101 Committee on Animal Use (CEUA) of UNIFESP under the register 9034130216.

102

103 **2.2. Induction of COPD and Preparation of the cigarette smoke** 104 **extract (CSE).**

105 The *in vivo* COPD was induced in C57Bl/6 mice by inhaling smoke from 14 cigarettes for 60
106 days, 7 days/week, for 30 min. The smoke was pumped into a plastic box measuring 42 cm (length) × 28
107 cm (width) × 27 cm (height), where the animals were kept and passively inhaled the cigarette smoke. For
108 the *in vitro* experiments, the cigarette smoke extract (CSE) was prepared through the burning of 14
109 commercial cigarettes (tar: 13 mg; nicotine: 1.10 mg; carbon monoxide: 10 mg) using a vacuum machine
110 (Nevoni – 1001 VF-PE. Series: 304 - Brazil) with -11 Kpa to be incorporated into PBS.

111

112 **2.3. Oral feeding with *Lactobacillus rhamnosus***

113 The mice were treated via gavage with probiotic *Lactobacillus rhamnosus* (*Lr*) (1×10^9 CFU/0.2
114 mL PBS/mouse) (Liane Laboratory, Ribeirão Preto, SP) each day for seven days prior to the COPD
115 induction and then 3 times/week until euthanasia. The experimental protocol is illustrated in Figure 1.

116

117 **Fig 1. Time schedule of COPD model and probiotic treatment.** Male C57Bl/6 mice were exposed to
118 inhalation of cigarette smoke (14 cigarettes; 30 minutes/day; 7 days/week; during 60 days) for COPD
119 induction and treated with *Lactobacillus rhamnosus* (*Lr*) (10^9 CFU/0.2 mL PBS/mouse) for seven days
120 prior to the COPD induction and, after that, 3 times/week until the day of the euthanasia.

121

122 **2.4. Murine bronchial epithelial cells and culture conditions.**

123 The lungs were removed and immersed in sterile enzymatic solution for digestion with dispase II
124 for 60 min. After digestion, the cells were resuspended in cell basal medium that contained growth factors
125 for epithelial cells and placed in petri dishes for 20 min. Adherent cells were collected and resuspended in

126 RPMI 1640 plus fetal bovine serum, penicillin, and streptomycin and then maintained in culture until the
127 third passage. The cells were stimulated with 2.5% cigarette smoke extract (CSE) incorporated into the
128 culture medium as detailed in subsection 2.4 (BEAS cells and culture condition). The treatment with
129 *Lactobacillus rhamnosus* (*Lr*) was performed 1 h before CSE addition in culture medium with murine
130 bronchial epithelial cells. Then 24 hours after CSE addition, the culture supernatants were removed, and
131 stored at -40°C until use.

132

133

134 **2.5. Human bronchial epithelial cells (BEAS-2B) and culture** 135 **conditions.**

136 The lineage of human bronchial epithelium cells (BEAS-2B (ATCC® CRL-9609™)) were
137 isolated from normal human bronchial epithelium obtained from autopsy of healthy individuals and were
138 acquired from American Type Culture Collection (Manassas, VA). BEAS cells were cultured in small
139 airway cell basal medium that contained growth factors for epithelial cells. The cells used were between
140 the 45th and 55th generation passages. BEAS cells were washed with medium and introduced into each
141 well of 24-well culture plates in triplicate at a concentration of 6×10^5 cells.mL⁻¹. After 12 hours, BEAS
142 cells were exposed to cigarette smoke extract (CSE) and probiotic (1×10^5 UFC of *Lr*). The CSE was
143 made from 1 unfiltered cigarette which was burned in 10 mL of culture medium. A vacuum pump was
144 used at a pressure of -11 Kpa so that the cigarette smoke could be incorporated into the culture medium.
145 Cells were stimulated with 2.5% CSE incorporated into the culture medium. The treatment with probiotic
146 was performed 1 h before CSE addition in culture medium with BEAS cells. Then, 24 hours after CSE
147 addition, the culture supernatants were removed, and stored at -40°C until use.

148

149

150 **2.6. Experimental Groups**

151 The animals were randomly divided into 3 groups of 7 animals each: control (pure air inhalation
152 for 60 days); COPD (14 cigarettes smoke inhalation for 60 days; 30 min a day; 7 days/week); *Lr* + COPD
153 (14 cigarettes smoke inhalation for 60 days; 30 min a day, 7 days/week + *Lactobacillus rhamnosus*). The
154 animals received *Lr* (10^9 CFU/0.2 mL PBS/mouse) every day for the entire week before inhalation of CS

155 and, after that, 3 days/week until euthanasia. For *in vitro* assays, murine bronchial epithelial cells or
156 BEAS cells were divided in 3 groups: control (culture medium alone), COPD (murine bronchial epithelial
157 cells or BEAS cells exposed to CSE), and *Lr* + COPD (murine bronchial epithelial cells or BEAS cells
158 exposed to *Lr* 1-hour prior to addition of CSE in culture medium). The murine bronchial epithelial cells
159 or BEAS cells were incubated with a density of 5×10^5 /mL of *Lr*.

160

161 **2.7. Bronchoalveolar lavage fluid (BALF)**

162 After the mice were euthanized with excess anesthetics, the trachea was cannulated, and lungs
163 were rinsed with 0.6 mL of cold PBS (saline). This was followed by 2 additional washings with the same
164 saline volume. Total and differential cell counts of BALF were determined by hemocytometer and
165 cytopsin preparation stained with Instant-Prov (Newprov, Brazil). Number of eosinophils, macrophages,
166 neutrophils, and lymphocytes were scored by light microscopy.

167

168 **2.8. Histology and image analysis**

169 After the euthanasia, the lungs were carefully removed, perfused, and fixed with 4%
170 paraformaldehyde for 24 h at a positive pressure (20 cm H₂O), for histological examination. Paraffin
171 (Sigma-Aldrich Co., St. Louis, MO, USA) was used to embed the fixed tissue. Lung segments of
172 approximately 5µm were stained with hematoxylin and eosin (Sigma-Aldrich Co.) for morphometric
173 analysis of pulmonary emphysema. The parameters analyzed were alveolar wall enlargement (Lm),
174 peribronchial inflammation, deposition of collagen fibers, and destruction of elastic fibers. Five airways
175 of all animals were imaged at 400 X magnifications using a Nikon Eclipse E-200 microscope camera and
176 the software Image Pro-Plus 4.0.

177

178 **2.8.1. Alveolar enlargement**

179 Sections of lung tissue were stained with hematoxylin and eosin (Sigma-Aldrich Co.), and the
180 increased air space was evaluated by the linear mean of the alveolar intercept (Lm) in twenty fields
181 selected from each slide of lung tissue, with amplification of 200 X. The destruction of the alveolar septa
182 was evaluated by the technique of counting points in twenty fields randomly throughout the pulmonary
183 parenchyma (excluding fields presenting airways and pulmonary vessels).

184

185

186

187 ***2.8.2. Peribronchial Inflammation***

188 Peribronchial inflammation was obtained through analyzing the space between the basal
189 membrane and adventitia. The number and type of cells (mononuclear and polymorphonuclear) were
190 evaluated in this specific area. The results were expressed as number of cells per square millimeter.
191 Neutrophils were counted according to morphological criteria; groups were blinded. The number of
192 neutrophils per square millimeter of lung tissue was presented.

193

194 ***2.8.3. Collagen Fibers***

195 The collagen deposition in the airways was performed with the addition of Picrosirius staining
196 (Sigma-Aldrich Co.). The density of the collagen fibers was measured using a standardized color
197 threshold (red) by the CellSens software from the region between the basal membrane of the epithelium
198 to the adventitial airway. The results were expressed as μm^2 of collagen fibers/collagen per μm^2 of lung
199 tissue area.

200

201 ***2.8.4. Elastic Fibers***

202 The destruction of elastic fibers in the airways was performed with the addition of Verhoeff Van
203 Grieson (Sigma-Aldrich Co.) staining for elastic fiber marking. In brief, five airway tissues per animal
204 (all animals of all groups) were subjected to image analysis using the CellSens software. The density of
205 the elastic fibers was measured using a standardized color threshold (brown) by the CellSens software for
206 the region between the basal membrane of the epithelium to the adventitial airway. The results were
207 expressed in μm^2 of elastic fibers/elastic fibers per μm^2 of lung tissue area.

208

209 **2.9. Cytokines and TGF- β in BALF, in bronchial epithelial cells and** 210 **lung tissue**

211 The levels of cytokine, chemokines and TGF- β in BALF, in murine bronchial epithelial cells, as
212 well as in BEAS cells were assessed using ELISA kits for mice or human. The ELISA assay kit for mice

213 was also employed to measure the SOCS3 concentration in lung tissue. All ELISA kits were used in
214 accordance with the manufacturer's instructions. Values are expressed as pg/mL deduced from standard
215 runs in parallel with recombinant cytokines, chemokines and TGF- β .

216

217 **2.10. Real-Time Polymerase Chain Reaction (PCR) for MMP-9,** 218 **MMP-12, TIMP1, TIMP2, TLR2, TLR4, TLR9, NF- κ B, STAT3 and** 219 **SOCS3**

220 The mRNA expression in the animal lung tissue, in murine bronchial epithelial cells, as well as in
221 BEAS cells was quantified by real-time PCR for MMP-9: CGGATTTGGCCGTAT TGGGC (forward)
222 and TGATGGCATGCACTGTGGTC (reverse) and MMP-12: TTTGACCCACTTCGCC (forward) and
223 GTGACACGACGGAACAG (reverse), TIMP-1: CCACGAATCAAGAGACC (forward) and
224 GGCCCGTGATGAGAAAC (reverse) and TIMP-2: GGTAGCCTGTGAATGTTCTT (forward) and
225 ACGAAAATGCCCTCAGAAG (reverse), TLR-2: GAGCATCCGAATTGCATCACC (forward) and
226 CCCAGAAGCATCACATGACAGAG (reverse), TLR-4: CATGGATCAGAACTCAGCAAAGTC
227 (forward) and CATGCCATGCCTTGTCTTCA (reverse), and TLR-9: CAGCTAAAGGCCCTGACCAA
228 (forward), and CCACCGTCTTGAGAATGTTGTG (reverse), plus the transcription factors NF- κ B:
229 CCGGGAGCCTCTAGTGAGAA (forward) and TCCATTTGTGACCAACTGAACGA (reverse),
230 STAT3: TACCAGCCCTCCAATCAAAG (forward) and GGTCACACAGCACACAATCC, and SOCS3:
231 CTGCAGGAGAGCGGATTCTACT (forward) and GCTGTGCGGGATAAGAAAGG (reverse). The
232 tests were conducted in accordance with the manufacturer's specifications. Briefly, 1 μ g of the total RNA
233 was used for cDNA synthesis. Reverse transcription (RT) was performed in a 200 μ L solution in the
234 presence of 50mM Tris-HCl (pH 8.3), 3mM MgCl₂, 10mM dithiothreitol, 0.5mM dNTPs, and 50ng
235 random oligonucleotides with 200 units of reverse transcriptase (Invitrogen™). Reaction conditions
236 were: 20 °C for 10 min, 42 °C for 45 min, and 95 °C for 5 min. A 7000-sequence detection system (ABI
237 Prism, Applied Biosystems®) was used through the SYBRGreen kit (Applied Biosystems®) and the
238 values obtained normalized against the internal control gene GAPDH: CGGATTTGGCCGTATTGGGC
239 (forward) and TGATGGCATGCACTGTGGTC (reverse).

240

241

242

243 **2.11. Immunohistochemistry for NF- κ B and STAT3 in lung tissue.**

244 For immunohistochemistry analysis, the paraffin-embedded sections of lung tissues were
245 deparaffinized with xylene and then rehydrated. Section slides were incubated with 3% hydrogen
246 peroxide for 10 min, then in 5% BSA in PBS blocking solution for 20 min, and after, incubated overnight
247 with anti-NF- κ B antibody (Cell signaling Technology) in blocking solution at 4 °C. After washing with
248 PBS, the slides were treated with biotinylated secondary antibody for 20 min, streptavidin-HRP
249 (horseradish peroxidase) for 20 min, and 3,3N-Diaminobenzidine Tetrahydrochloride for 10 min. The
250 slides were then washed, and counter stained with hematoxylin. Slides were evaluated by microscopy,
251 and the positive cells exhibited yellow or brown particles.

252

253 **2.12. Statistics**

254 The results were evaluated through the Analysis of Variance (ANOVA) and the Tukey-Kramer
255 Multiple Comparison Test to determine the differences between the groups. The analysis were performed
256 using Sigma Stat 3.1 software and graphs using GraphPad Prism 5.0 software. The results were
257 considered significant when $p < 0.05$.

258

259 **3. Results**

260 **3.1. *Lactobacillus rhamnosus* attenuate the cigarette-induced airway** 261 **inflammation**

262 The analysis of cellular content in BALF revealed that in response to cigarette smoke, the COPD
263 group presented with an increase in the total number of cells in the airways, in comparison to the control,
264 non-smoking group (Figure 2A). In concordance with the characteristic inflammatory response observed
265 in COPD manifestation, the infiltrating cells were constituted by macrophages (2B), neutrophils (2C), and

266 lymphocytes (2D). In contrast, it is possible to observe in the *Lr* group that probiotic feeding inhibited
267 the influx of inflammatory cells into the airways. This phenomenon was accomplished by a significant
268 attenuation in the levels of pro-inflammatory molecules (Figure 3). The exposure to cigarette smoke
269 increased the levels of both pro-inflammatory cytokines, such as IL-1 β (3A), IL-6 (3B), TNF- α (3C), KC
270 (3D), IL-17 (3E), and TGF- β (3J) in BALF, in comparison to control group. Controversially, the *Lr* group
271 presented with a significant reduction in the levels of both pro-inflammatory cytokines and chemokines
272 when compared with the COPD mice. For notice, the inflammatory response observed in the COPD
273 group was correlated with a significant reduction in the levels of IL-10 (3K) in the airways, whereas in
274 the *Lr* this anti-inflammatory cytokine is increased.

275

276 **Fig 2. Leukocyte lung infiltration.** After exposure of C57Bl/6 male mice to cigarette smoke and
277 treatment with *Lactobacillus rhamnosus* (*Lr*), the total cells (2A) and inflammatory cells were counted
278 ($\times 10^5$) in BALF in millimeters by the morphometric evaluations of cytopsin preparations. Pulmonary
279 inflammation was represented by the influx of specific leukocytes; neutrophil (2B), macrophage (2C), and
280 lymphocytes (2D) in BALF fluid. All cell counts were obtained from the control, COPD and *Lr* + COPD
281 groups. Each plot represents mean \pm SEM from 7 different animals. The experiments were performed in
282 triplicate. Results were considered significant when $p < 0.05$.

283

284 **Fig 3. Cytokines and chemokines in BALF and SOCS3 in lung tissue.** The BALF obtained from
285 control, COPD, and *Lr* + COPD groups was prepared for analysis of pro- and anti-inflammatory
286 cytokines. The mediator's TNF (3A), IL-1 β (3B), IL-6 (3C), IL-17 (3D), CXCL1 (3E), IL-10 (3F), TGF- β
287 (3G) in BALF and SOCS3 (3H) in lung tissue were assayed by enzyme-linked immunosorbent assay
288 (ELISA). Each plot represents mean \pm SEM from 7 different animals. The experiments were performed in
289 triplicate. Results were considered significant when $p < 0.05$

290

291 **3.2. *Lactobacillus rhamnosus* attenuates pulmonary remodeling.**

292 In concordance with the findings observed in the BALF, the COPD group presented with an
293 inflammatory response in lung tissue (Figure 4), with marked influx of neutrophils into the parenchyma

294 (4A). Also, these animals exhibited signals characteristic of tissue remodeling as alveolar wall
295 enlargement (4B), and collagen (4C) and elastic fibers deposition (4D).

296
297 **Fig 4. Airway morphometry.** After exposure of C57Bl/6 male mice to cigarette smoke and treatment
298 with *Lactobacillus rhamnosus* (*Lr*), sections (5 μ m) of formalin-fixed lungs were stained with
299 hematoxylin and eosin for histological examination in control, COPD, and *Lr* + COPD groups. (Original
300 magnification, $\times 200$). (4A) Quantification of neutrophils in airway wall, (4B) Alveolar enlargement (Lm),
301 (4C) Collagen fibers deposition, and (4D) Fiber elastics destruction were measured as described in
302 Material and Methods section. Each plot represents mean \pm SEM from 7 different animals. Results were
303 considered significant when $p < 0.05$.

304
305 **3.3. *Lactobacillus rhamnosus* modulates the balance between**

306 **metalloproteases and tissue inhibitors of metalloproteases**

307 In COPD, pulmonary remodeling is correlated with the deregulation in the balance between MMP
308 and its inhibitors (TIMP). The analysis of lung tissue by quantitative PCR revealed that CS inhalation
309 induced a significant increase in the mRNA expression of both MMP-9 (5A) and MMP-12 (5B)
310 accomplished by inhibition in the expression of the genes associated with TIMP-1 and TIMP-2 proteins
311 (5C and 5D, respectively). On the other hand, oral feeding with *Lr* sustained the expression of the mRNA
312 for MMP-9 and MMP-12 in levels comparable to those found in control animals, and partially restored
313 the expression of both TIMP-1 and TIMP-2 genes.

314
315 **Fig 5. Metalloproteases in lung tissue.** The mRNA expression of the MMP-9, MMP-12, TIMP-1 and
316 TIMP-2 in lung from the control, COPD, and *Lr* + COPD groups is illustrated. After exposure of C57Bl/6
317 male mice to cigarette smoke and treatment with *Lactobacillus rhamnosus* (*Lr*), the mRNA expression for
318 MMP-9 (5A), MMP-12 (5B), TIMP-1 (5C), and TIMP-2 (5D) in lung tissue were evaluated through Real
319 Time-PCR. The values were normalized by the GAPDH expression and expressed by arbitrary units.
320 Each bar represents mean \pm SEM from 7 different animals. The experiments were performed in triplicate.
321 Results were considered significant when $p < 0.05$.

322
323

324 **3.4. *Lactobacillus rhamnosus* downregulates expression of STAT3** 325 **and NF- κ B in lung tissue**

326 The activation of the STAT3 pathway and, consequently, the induction of NF- κ B transcription factor
327 regulate the expression of genes associated with inflammation in lung diseases and are correlated with
328 disease severity. In concordance, inhalation of CS induced a significant increase in the mRNA expression
329 of NF- κ B and STAT3-related genes in lung tissue from COPD mice, in comparison to control group
330 (Figures 6A and 6B, respectively). In contrast, the *Lr* group presented with a lower expression of these
331 genes when compared to COPD mice, in levels similarly to those found in control group. These data were
332 corroborated with immunohistochemical staining of lung tissue (Figure 6A and 6B).

333

334

335 **Fig 6. Transcription factors in lung tissue.** The mRNA expression of the NF- κ B and STAT3 in lung
336 from the control, COPD, and *Lr* + COPD groups is illustrated. After exposure of C57Bl/6 male mice to
337 cigarette smoke and treatment with *Lactobacillus rhamnosus* (*Lr*), the mRNA expression for NF- κ B (6A)
338 and STAT3 (6B) in lung tissue were evaluated through Real Time-PCR. The values were normalized by
339 the GAPDH expression and expressed by arbitrary units. For immunohistochemical localization of NF-
340 κ B and STAT3 in lung tissue of mice from control, COPD and *Lr* + COPD groups, the positive reaction
341 was visualized as a yellowish-brown stain. Each plot represents mean \pm SEM from 7 different animals.
342 Results were considered significant when $p < 0.05$.

343

344 **3.5. The beneficial effect of *Lactobacillus rhamnosus* is associated** 345 **with a reduction in the expression of Toll-like receptors in lungs**

346 Because TLR engagement plays an important role in COPD pathogenesis, we decided to determine the
347 status of mRNA expression to different TLRs in our model. Figure 7 demonstrates that among the TLR
348 studied, the expression of mRNA for TLR2 (7A), TLR4 (7B), and TLR9 (7C) increased in cigarette
349 smoke challenged-mice compared to control group. On the other hand, the treatment with *Lr* reduced the
350 expression of induced a significant reduction in these genes in comparison with COPD group.

351

352 **Fig 7. Toll-like receptors in lung tissue.** After exposure of C57Bl/6 male mice to cigarette smoke and
353 treatment with *Lactobacillus rhamnosus* (*Lr*), the mRNA expression for TLR2 (7A), TLR4 (7B) and
354 TLR9 (7C) in lung tissue of control, COPD and *Lr* + COPD groups was evaluated through Real Time-
355 PCR. The values were normalized by the GAPDH expression and expressed by arbitrary units. Each bar
356 represents mean \pm SEM from 7 different animals. The experiments were performed in triplicate. Results
357 were considered significant when $p < 0.05$.

358

359 **3.6. *Lactobacillus rhamnosus* modulates the secretion of** 360 **inflammatory mediators in murine bronchial epithelial cells**

361 The airway epithelium is central to the pathogenesis of COPD. Therefore, we investigated the
362 secretion of cytokines and chemokines from murine bronchial epithelial cells stimulated with CSE,
363 treated with *Lr*, or stimulated with CSE and treated with *Lr*. As shown in figure 8, the secretion of TNF
364 (8A), IL-1 β (8B), IL-6 (8C), CXCL1 (8D), from CSE-bathed murine bronchial epithelial cells increased
365 compared to control group. On the contrary, the CSE-exposed murine bronchial epithelial cells secreted
366 lower levels of IL-10 (8E), TGF β (8F) as well as SOCS3 (8G) than murine bronchial epithelial cells from
367 control group. The pre-incubation with *Lr* probiotic inhibited the secretion of all cytokines, with
368 exception of SOCS3, TGF β and IL-10, which were upregulated, even in comparison to control group.

369

370 **Fig 8. Murine bronchial epithelial cells.** Cytokines and chemokines secretion from murine bronchial
371 epithelial cells of control and COPD groups and treated with *Lr* 1 hour before addition of CSE is
372 illustrated in figure 8. The inflammatory mediator's TNF (8A), IL-1 β (8B), IL-6 (8C), CXCL1 (8D), IL-
373 10 (8E), TGF- β (8F) and SOCS3 (8G) in supernatant of murine bronchial epithelial cells were assayed by
374 enzyme-linked immunosorbent assay (ELISA). The assays were performed in triplicate Results were
375 considered significant when $p < 0.05$.

376

377

378

379 **3.7. *Lactobacillus rhamnosus* modulates the secretion of** 380 **inflammatory mediators in human bronchial epithelial cells (BEAS).**

381 We investigated the secretion of cytokines and chemokines from human bronchial epithelial cells
382 (BEAS) stimulated with CSE or stimulated with CSE and treated with *Lr*. As shown in figure 9, the
383 secretion of TNF (9A), IL-1 β (9B), IL-6 (9C), and CXCL8 (9D) from CSE-bathed BEAS cells increased
384 compared to control group. On the other hand, CSE-exposed BEAS cells secreted lower levels of IL-10
385 (9E) as well as TGF β (9F) compared to control group. The same effect was observed with levels of
386 SOCS3 (9G) The presence of probiotic in BEAS cell culture stimulated with CSE markedly inhibited the
387 secretion of all cytokines investigated herein, with exception of SOCS3, TGF β and IL-10, which were
388 upregulated in comparison to control cells.

389
390 **Fig 9. Human bronchial epithelial cells (BEAS).** Cytokines and chemokines secretion from BEAS cells
391 stimulated with CSE and treated with *Lr* are illustrated in figure 9. The inflammatory mediator's TNF
392 (9A), IL-1 β (9B), IL-6 (9C), CXCL8 (9D), IL-10 (9E), TGF β (9F) and SOCS3 (9G) in supernatant of
393 human bronchial epithelial cells were assayed by enzyme-linked immunosorbent assay (ELISA). The
394 assays were performed in triplicate. Results were considered significant when $p < 0.05$.

395

396 **3.8. *Lactobacillus rhamnosus* downregulates NF- κ B, STAT3 and** 397 **SOCS3 in murine bronchial epithelial cells and in BEAS cells.**

398 The *in vivo* findings indicated that the anti-inflammatory effects of *Lr* treatment was associated
399 with the modulation of the genes associated with NF κ B and STAT3 pathways (Figure 10). In
400 concordance, both the murine bronchial epithelial cells (10A and 10B) and human bronchial epithelial
401 cells (10C and 10D) cells presented with increased expression of mRNA to NF- κ B and STAT3 genes
402 upon exposure to CSE, in comparison to control cells. The *Lr* treatment maintained the expression of
403 these genes at levels similar to those observed in the control cells, corroborating the notion that the
404 beneficial effects associated with the probiotic involves the control of the STAT3 pathway. On the
405 contrary, both the murine bronchial epithelial cells (10C) and the BEAS cells (10F) stimulated with CSE

406 presented a level lower of SOCS3 compared to control group. The oral feeding with *Lr* restored the
407 SOCS3 levels in murine bronchial cells as well as in BEAS cells to values similar to control. STAT3 and
408 NFκB pathways are regulated by molecules such as SOCS3, which lower levels has been associated with
409 COPD.

410

411

412 **Fig 10. Transcription factors in murine bronchial epithelial cells and in BEAS.** The mRNA
413 expression of the NF-κB, STAT3 as well as SOCS3 in murine bronchial epithelial cells from the control,
414 COPD, and *Lr* + COPD groups is illustrated in figure 10A, 10B and 10C, respectively. Figures 10D, 10E
415 and 10F presents the mRNA expression of the NF-κB, STAT3 as well as SOCS3 in human bronchial
416 epithelial cells (BEAS) from the control, COPD, and *Lr* + COPD groups. After exposure of both airway
417 epithelial cells, murine and human, to cigarette smoke extract (CSE) and treatment with *Lactobacillus*
418 *rhamnosus* (*Lr*), the mRNA expression for NF-κB, STAT3 and SOCS3 in lung tissue was evaluated
419 through Real Time-PCR. The values were normalized by the GAPDH expression and expressed by
420 arbitrary units. The assays were performed in triplicate. Results were considered significant when $p <$
421 0.05.

422

423 **4. Discussion**

424 The present study demonstrates the ability of the probiotic *Lactobacillus rhamnosus* (*Lr*) to
425 control lung inflammation in cigarette smoke (CS)-induced COPD experimental model. *Lr* feeding
426 attenuated both the migration of inflammatory cells to the lung and tissue remodeling features, such as
427 alveolar enlargement and exacerbated deposition of collagen and mucus secretion. Although the
428 mechanisms involved in this phenomenon remain an object of study, the probiotic mitigated the cytokine
429 storm associated with COPD pathogenesis, maintaining the equilibrium between transcription factors that
430 regulate the production of pro and anti-inflammatory molecules.

431 Our findings corroborate previous studies showing that that CS inhalation induces a robust migration of
432 inflammatory cells to the lung environment, mainly macrophage and neutrophils [41-43]. In response to
433 CS, pulmonary cells produced pro-inflammatory cytokines such as IL-1β, IL-6 and TNF-α resulting in the
434 secretion of several chemokines. The increase in CXCL1 levels promotes the migration and

435 differentiation of monocytes in lung tissue, amplifying the inflammatory process [44-46]. The chronic
436 inflammation of the lungs results in alterations in the parenchyma architecture, a process known as tissue
437 remodeling, due an unbalance between active MMPs and its inhibitors, TIMP [47, 48]. In concordance
438 with this notion, CS group presented, in association with pulmonary neutrophilia, alveolar enlargement as
439 well as loss of alveolar parenchyma, collagen deposition, and destruction of elastic fibers. These
440 structural alterations were accomplished by a significant increase in the mRNA expression for MMP-9
441 and MMP-12 that was inversely to gene expression for TIMP-1 and TIMP-2. Despite the
442 cytokine/chemokine storm and the consequent cascade of events induced by CS inhalation, probiotic
443 feeding attenuated the inflammatory process both in the airways space and lung parenchyma.
444 Although the mechanisms behind this effect are allusive, we found that *Lr* feeding increased both the
445 levels of IL-10 in the BALF and SOCS3 in lung tissue, even when compared to control animals,
446 indicating that probiotic induced an anti-inflammatory steady state. This idea is corroborated by the fact
447 that *Lr* feeding sustained the levels of mRNA for TLRs, one of the major players in CS-induced COPD,
448 and for pro-inflammatory transcription factors, such as NFκB and STAT3, at levels comparable to those
449 from control animals.

450 Because epithelial cells are the interface between innate and adaptive immunity and a growing body of
451 evidence supports a major role for non-immune pulmonary cells in COPD [51-53], we decided to study
452 the response of epithelial cells to probiotic stimulation. The exposure of murine or human epithelial cells
453 to cigarette extract (CSE) resulted in the secretion of several pro-inflammatory cytokines and chemokines
454 and induced expression of mRNA to STAT3 and NFκB, mirroring the observed in the *in vivo* model. In
455 contrast, probiotic stimulation made the epithelial cells refractory to the inflammatory provocation
456 provided by CE.

457 The proposal of action mechanism for *Lr* effect in which the bronchial epithelium is the important target
458 was confirmed when the probiotic modulated the secretion of pro- and anti-inflammatory cytokines in
459 human bronchial epithelial cells stimulated with CSE. Moreover, our results show that the anti-
460 inflammatory effect of *Lr* on cytokines secretion from CSE-exposed human bronchial epithelial cells was
461 due to the downregulation of both transcription factors, NF-κB and STAT3. The modulation of
462 transcription factors SOCS3 and STAT3 by probiotic was also observed in human bronchial epithelial
463 cells. This reinforces the idea that the *in vivo* action mechanism of *Lr* involves the signaling pathway NF-

464 κ B/STAT3/SOCS3 in human bronchial epithelium cells in order to attenuate both the lung inflammation
465 and the exacerbation of immune response in lung microenvironment.
466 Finally, several strains of *Lactobacillus*, as well as its structural components, and microbial-produced
467 metabolites can stimulate epithelial cell signaling pathways which can prevent cytokine and oxidant-
468 induced epithelial damage thereby promoting cell survival through increased production of cytoprotective
469 molecules [54]. Our results demonstrated that *Lr*, by itself, increased secretion of both the IL-10 and the
470 TGF- β secretion as well as SOCS3 levels in human bronchial epithelial cells unstimulated with CSE,
471 which supports the idea that daily supplementation with probiotic may protect the lung milieu through of
472 airway epithelial cells, since the IL-10 can suppress pro-inflammatory genes and the TGF- β can guarantee
473 the integrity of airway epithelial barrier.
474 In conclusion, the present manuscript describes by the first time that *Lr* modulates the secretion of pro-
475 and anti-inflammatory molecules from human airway epithelial cells through of restoring the equilibrium
476 between the transcription factors NF- κ B/STAT-3 and SOCS3, and it seems to be an important action
477 mechanism of probiotic in order to control lung inflammation as well as airway remodeling in COPD.

478

479 **5. References**

- 480 [1] Hou WR, Hou YL, Wu GF, Song Y, Su XL, Sun B, et al. cDNA, genomic sequence cloning and
481 overexpression of ribosomal protein gene L9 (rpL9) of the giant panda (*Ailuropoda melanoleuca*). *Genet*
482 *Mol Res.* 2011;10: 1576-1588.
- 483 [2] Global Strategy for the Diagnosis, Management, and prevention of Chronic Obstructive Pulmonary
484 Disease. 2019.
- 485 [3] D.D. Wu, J. Song, S. Bartel, S. Krauss-Etschmann, M.G. Rots, M.N. Hylkema. The potential for
486 targeted rewriting of epigenetics marks in COPD as a new therapeutic approach. *Pharmacology &*
487 *Therapeutics.* 17 (2017) 30217-30226.
- 488 [4] T.J. Haw, M.R. Starkey, S. Pavlidis, M. Fricker, A.L. Arthurs, P.M. Nair, et al. Tolle-like receptor 2
489 and 4 opposing roles in the pathogenesis of cigarette smoke-induced chronic obstructive pulmonary
490 disease. *Am J Physiol Lung Cell Mol Physiol.* (2017).

494

495 [5] P. J. Barnes. Cellular and molecular mechanisms of Ashtma and COPD. *Clinical Science*. 131 (2017)

496 1541-1558.

497

498 [6] M.K. Han, A. Agusti, P.M. Calverley, B.R. Celli, G. Criner, J.L. Curtis, et al. Chronic Obstructive

499 Pulmonary Disease phenotypes. *Am J Respir Crit Care Med*.182 (2010) 598-604.

500

501 [7] C.M. Freeman, F.J. Martinez, M.K. Han, G.R. Washko Jr, A.L. McCubrey, S.W. Chensue, et al. Lung

502 CD8+ T cells in COPD have increased expression of bacterial TLRs. *Respiratory Research*. 14 (2013) 1-

503 13.

504

505 [8] R.M Tuder, I. Petrache. Pathogenesis of Chronic Obstructive Pulmonary Disease. *The Journal of*

506 *Clinical Investigation*. 122 (2012) 2749-2755

507

508 [9] M.C. Lebre, T. Burwell, P.L. Vieira, J. Lora, A.J. Coyle, M.L. Kapfenberg, et al. Differential

509 expression of inflammatory chemokines by Th1- and Th2-cell promoting dendritic cells: a role for

510 different mature dendritic cell populations in attracting appropriate effector cells to peripheral sites of

511 inflammation. *Immunology and Cell Biology*. 83 (2005) 525-535.

512

513 [10] J. Pons, J. Sauleda, V. Regueiro, C. Santos, M. Lopez, J. Ferrer, et al. Expression of toll-like receptor

514 2 is up regulated in monocytes from patients with chronic obstructive pulmonary disease. *Respiratory*

515 *Research*. 107 (2006) 1-9

516

517 [11] J.L Simpson T.V. Grissel, J. Douwes, R.J. Scott, M.J. Boyle, P.G. Gibson. Innate immune activation

518 in neutrophilic asthma and bronchiectasis. *Thorax*. 62 (2007) 211-218.

519

520 [12] P.M. Hansbro, T.J. Haw, M.R. Starkey, K. Miyake. Toll-like receptors in COPD. *Eur Respir J*. 49

521 (2017) 1-3.

522

523 [13] R.F. Foronjy, M.A. Salathe, A.J. Dabo, N. Baumlin, N. Cummins, N. Eden, et al. TLR9 expression is

524 required for the development of cigarette smoke-induced emphysema in mice. *Am J Physiol Lung Cell*

525 *Mol Physiol*. 311 (2016) 154-166.

526

- 527 [14] C.M. Freeman, J.L. Curtis, S.W. Chensue. CC chemokine receptor 5 and CXC chemokine receptor 6
528 expression by lung CD8+ cells correlate with Chronic Obstructive Pulmonary Disease severity. The
529 American Journal of Pathology. 171 (2007) 767-776.
- 530
531 [15] W. Gao, L. Lingling, Y. Wang, S. Zhang, I.M. Adcock, P.J. Barnes, et al. Bronchial epithelial cells:
532 the key effector cells in the pathogenesis of chronic obstructive pulmonary disease? *Respirology*. 20
533 (2015) 722-729.
- 534
535 [16] Z. Navratilova, V. Kolek, M. Petrek. Matrix metalloproteinase and their inhibitors in chronic
536 obstructive pulmonary disease. *Arch Immunol Ther Exp*. 64 (2016) 177-193.
- 537
538 [17] R. Chadhuri, C. McSharry, M. Spears, J. Brady, C. Grierson, C.M. Messow, et al. Sputum matrix
539 metalloproteinase-9 is associated with the degree of emphysema on computed tomography in COPD.
540 *Translational Respiratory Medicine*. 1 (2013) 1-5.
- 541
542 [18] A. Noguera, C. Gomez, R. Faner, B. Cosio, A. Gonzalez-Periz, J. Claria, et al. An investigation of
543 the resolution of inflammation (catabasis) in COPD. *Respiratory Research*. 13 (2012) 1-9.
- 544
545 [19] S. Kwiatkowska, K. Noweta, M. Zieba, D. Nowak, P. Bialasiewicz. Enhanced exhalation of matrix
546 metalloproteinase-9 and tissue inhibitor of metalloproteinase-1 in patients with COPD exacerbation: a
547 prospective study. *Respiration*. 84 (2012) 231-241.
- 548 [20] N. Nasreen, L. Gonzalves, S. Peruvemba, K.A. Mohammed. Fluticasone furoate is more effective
549 than mometasone furoate in restoring tobacco smoke inhibited SOCS-3 expression in airway epithelial
550 cells. *Int Immunopharmacol*. 19 (2014) 153-160.
- 551
552 [21] C.M. Prelê, E. Yao, R.J. O'Donogue, S.E. Mutsaers, D.A. Knight. Stat3: a central mediator of
553 pulmonary fibrosis? *Proc Am Thor Soc*. 9 (2012) 177-182.
- 554
555 [22] A.R. Almeida-Oliveira, J.C.J Aquino-Junior, A. Abbasi, A. Santos-Dias, M.C. Oliveira-Junior, R.W.
556 Alberca-Custodio, et al. Effects of aerobic exercise on molecular aspects of asthma: involvement of
557 SOCS-JAK-STAT. *Exercise Immunology Review*. 25 (2019) 50-62.
- 558

- 559 [23] S. McCormick, N. Gowda, J.X. Fang, N.M. Heller. Suppressor of cytokine signaling (SOCS)1
560 regulates interleukin-4 (IL-4)-activated insulin receptor substrate (IRS)-2 tyrosine phosphorylation in
561 monocytes and macrophages via the proteasome. *J Biol Chem.* 291 (2016) 20574-20587.
- 562
563 [24] H. Shoda, A. Yokoyama, R. Nishino, T. Nakashima, N. Ishikawa, Y. Haruta, et al. Overproduction
564 of collagen and diminished SOCS1 expression are causally linked in fibroblasts from idiopathic
565 pulmonary fibrosis. *Biochem Biophys Res Commun.* 353 (2007) 1004-1010.
- 566
567 [25] A. Apostolou, T. Kerenidi, A. Michopoulos, K.I. Gourgoulianis, M. Noutsias, A.E. Germenis, et al.
568 Association between TLR2/TLR4 gene polymorphisms and COPD phenotype in a Greek cohort. *Herz.* 8
569 (2016) 1-6.
- 570
571 [26] E. Mortaz, I.M. Adcock, K. Ito, A.D. Kraneveld, F.P. Nijkamp, G. Folkerts. Cigarette smoke induces
572 CXCL8 production by human neutrophils via activation of TLR9 receptor. *Eur Respir J.* 36 (2010) 1143-
573 1154.
- 574
575 [27] E. Mortaz, I.M. Adcock, F.L. Ricciardolo, M. Varahram, H. Jamaati, A.A. Velayati, G, et al. Anti-
576 Inflammatory Effects of *Lactobacillus Rahnmosus* and *Bifidobacterium Breve* on Cigarette Smoke
577 Activated Human Macrophages. *PLoS One.* 10 (2015) e0136455.
- 578
579 [28] L. Zuo, K. Lucas, C.A. Fortuna, C.C. Chuang, T.M. Best. Molecular Regulation of Toll-like
580 Receptors in Asthma and COPD. *Front Physiol.* 9 (2015) 312-315.
- 581
582 [29] T.A. Bhat, L. Panzica, S.G. Kalathil, Y. Thanavala. Immune Dysfunction in Patients with Chronic
583 Obstructive Pulmonary Disease. *Ann Am Thorac Soc.* 12 (2015) S169-S175.
- 584
585 [30] G.G. Brusselle, G.F. Joos, K.R. Bracke. New insights into the immunology of chronic obstructive
586 pulmonary disease. *Lancet.* 378 (2011) 1015-1026.
- 587
588 [31] M.A. Ponce-Gallegos, A. Ramirez-Venegas, R. Falfan-Valencia. Th17 profile in COPD
589 exacerbations. *International Journal of COPD.* 12 (2017) 1857-1865.
- 590

- 591 [32] G. Westergreen-Thorsson, M. Bagher, A. Andersson-Sjoland, L. Thiman, C.G. Lofdahl, O. Hallgren,
592 et al. VEGF synthesis is induced by prostacyclin and TGF- β in distal lung fibroblasts from COPD
593 patients and control subjects: implications for pulmonary vascular remodeling. *Respirology*. 32 (2017) 1-
594 8.
- 595
596 [33] J.C. Hogg. Pathophysiology of airflow limitation in chronic obstructive pulmonary disease. *The*
597 *Lancet*. 364 (2004) 709-721.
- 598
599 [34] G.T. Motz, B.L. Eppert, S. Guangyun, S.C. Wesselkamper, M.J. Linke, R. Deka, et al. Persistence of
600 lung CD8 T cell oligoclonal expansions upon smoking cessation in a mouse model of cigarette smoke-
601 induced emphysema. *The Journal of Immunology*. 181 (2008) 8036-8043.
- 602
603 [35] N. Hirota, J.G. Martin. Mechanisms of airway remodeling. *Chest*. 144 (2013) 1026-1032.
- 604
605 [36] J.L. López-Campos, W. Tan, J.B. Soriano. Global burden of COPD. *Respirology*. 21 (2016) 14-23.
- 606
607 [37] L.M. Rocha-Ramirez, R.A. Pérez-Solano, S.L. Castanon-Alonso, S.S.M Guerrero, A.R. Pacheco,
608 M.G. Garibay, et al. Probiotic *Lactobacillus* strains stimulate the inflammatory response and activate
609 human macrophages. *Journal of Immunology Research*. 5 (2017) 1-14.
- 610
611 [38] P. Forsythe. Probiotics and lung diseases. 139 (2011) 901-908.
- 612
613 [39] T. Kamiya, L. Wang, P. Forsythe, G. Goettsche, Y. Mao, Y. Wang, et al. Inhibitory effects of
614 *Lactobacillus reuteri* on visceral pain induced by colorectal distension in Sprague-Dawley rats. *Gut*. 55
615 (2006) 191-196.
- 616
617 [40] E.F. Verdú, P. Bercik, G.E. Bergonzelli et al. *Lactobacillus paracasei* normalizes muscle
618 hypercontractility in a murine model of postinfective gut dysfunction. *Gastroenterology*. 127 (2004) 826-
619 837.
- 620
621 [41] A.V. Rao, T.M. Bested, T.M. Beaulne, M.A. Katzman, C. Iorio, J.M Berardi, et al. *Gut Pathog*. 1
622 (2019) 6-10.
- 623

- 624 [42] S.D. Pouwels, G.J. Zijlstra, M. Van der Toorn, L. Hesse, R. Gras, N.H.T. Hacken, et al. Cigarette
625 smoke-induced necroptosis and DAMP release trigger neutrophilic airway inflammation in mice. *Am J*
626 *Physiol Lung Cell Mol Physiol.* 310 (2016) 377-386.
- 627
628 [43] K. Kruger, G. Dischereit, M. Seimetz, J. Wilhelm, N. Weissmann, F.C. Mooren. Time course of
629 cigarette smoke-induced changes of systemic inflammation and muscle structure. *Am J Physiol Lung Cell*
630 *Mol Physiol.* 309 (2015) 119-128.
- 631
632 [44] K.H. Lee, J. Jeong, Y.J. Koo, A.H. Jang, C.H. Lee, C.G. Yoo. Exogenous neutrophil elastase enters
633 bronchial epithelial cells and suppresses cigarette smoke extract-induced heme oxygenase-1 by cleaving
634 sirtuin 1. *J Biological Chemistry.* 33 (2017) 11-13.
- 635
636 [45] M. Bazett, A. Biala, R.D. Huff, M.R. Zeglinksi, P.M. Hansbro, M. Bosiljcic, et al. Attenuating
637 immune pathology using a microbial-based intervention in a mouse model of cigarette smoke-induced
638 lung inflammation. *Respir Res.* 18 (2017) 92-95.
- 639
640 [46] C. Costa, R. Rufino, S.L. Traves, J.R. Lapa Silva, P.J. Barnes, L.E. Donnelly. CXCR3 and CCR5
641 chemokines in induced sputum from patients with COPD. *Chest.* 133 (2008) 26-33.
- 642
643 [47] T. Inui, M. Watanabe, K. Nakamoto, M. Sada, A. Hirata, M. Nakamura, et al. Bronchial epithelial
644 cells produce CXCL1 in response to LPS and TNF α : A potential role in the pathogenesis of COPD. *Exp*
645 *Lung Res.* 44 (2018) 323-331.
- 646
647 [48] W. Hao, M. Li, Y. Zhang, C. Zhang, Y. Xue. Expressions of MMP-12, TIMP-4, and Neutrophil
648 Elastase in PBMCs and Exhaled Breath Condensate in Patients with COPD and Their Relationships with
649 Disease Severity and Acute Exacerbations. *J Immunol Res.* 17 (2019) 714-718.
- 650
651 [49] Z. Navratilova, V. Kolek, M. Petrek. Matrix Metalloproteinases and Their Inhibitors in Chronic
652 Obstructive Pulmonary Disease. *Arch Immunol Ther Exp (Warsz).* 64 (2016) 177-193.
- 653
654 [50] J.T. Ito, D.A.B. Cervilha, J.D. Lourenço, N.G. Gonçalves, R.A. Volpini, E.G. Caldini, et al.
655 Th17/Treg imbalance in COPD progression: A temporal analysis using a CS-induced model. *PLoS One.*
656 14 (2019): e0209351.

657

658 [51] D.A.B. Cervilha, J.T. Ito, J.D. Lourenço, C.R. Olivo, B.M. Saraiva-Romanholo, R.A. Volpini, et al.

659 The Th17/Treg Cytokine Imbalance in Chronic Obstructive Pulmonary Disease Exacerbation in an

660 Animal Model of Cigarette Smoke Exposure and Lipopolysaccharide Challenge Association.. *Sci Rep.* 13

661 (2019) 1921-1923.

662

663 [52] V. De Rose, K. Molloy, S. Gohy, C. Pilette, C.M. Greene. Airway epithelium dysfunction in cystic

664 fibrosis and COPD. *Mediators of Inflammation.* 21 (2018); 1-20.

665

666 [53] P.S. Hiemstra, P.B. McCray Jr, R. Bals. The innate immune function of airway epithelial cells in

667 inflammatory lung disease. *Eur Respir J.* 45 (2015) 1150-1162.

668

669 [54] I.H. Heijink, S.M. Brandenburg, D.S. Postma, A.J.M. van Oosterhout. Cigarette smoke impairs

670 airway epithelial barrier function and cell-cell contact recovery. *Eur Respir J.* 29 (2012) 419-428.

671

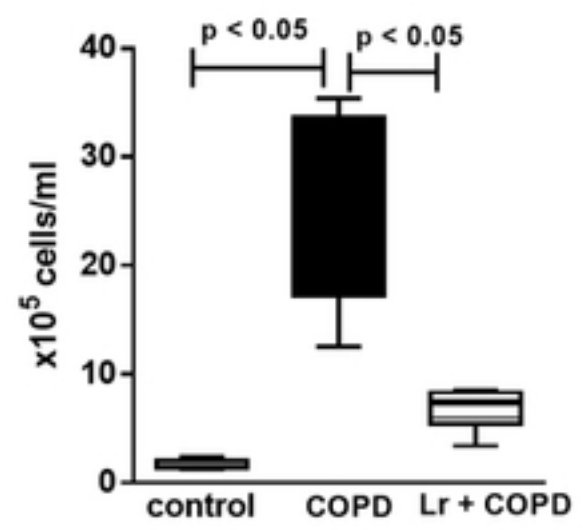
672 [55] K.Y. Sun, D.H. Xu, C. Xie, S. Plummer, J. Tang, X.F. Yang, X.H. Ji. *Lactobacillus paracasei*

673 modulates LPS-induced inflammatory cytokine release by monocyte-macrophages via the up-regulation

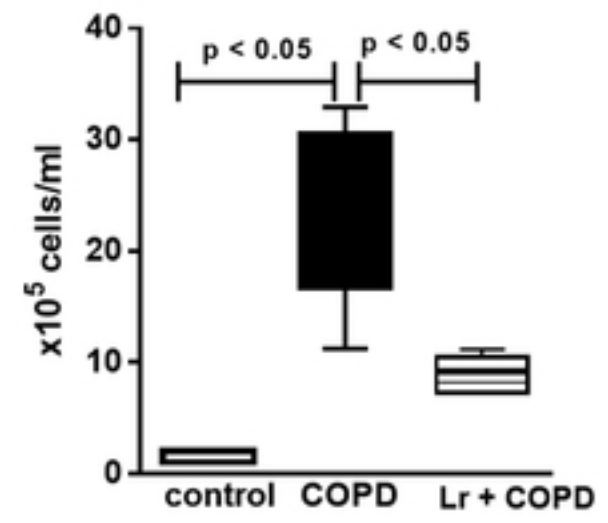
674 of negative regulators of NF-kappaB signaling in a TLR2-dependent manner. *Cytokine.* 92 (2017) 1-11.

Figure 2

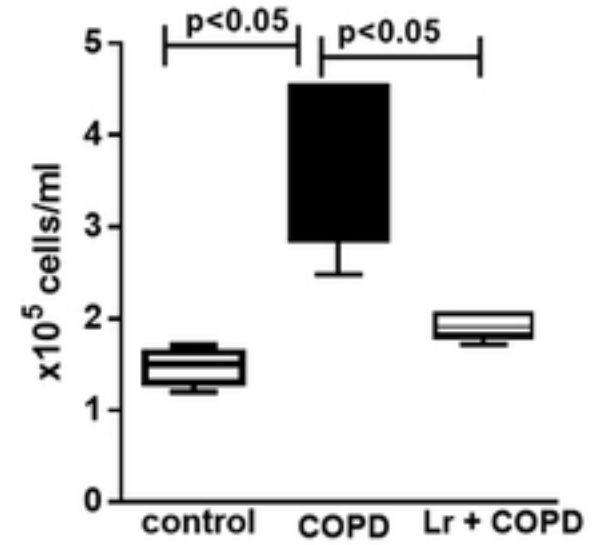
(2A)



(2B)



(2C)



(2D)

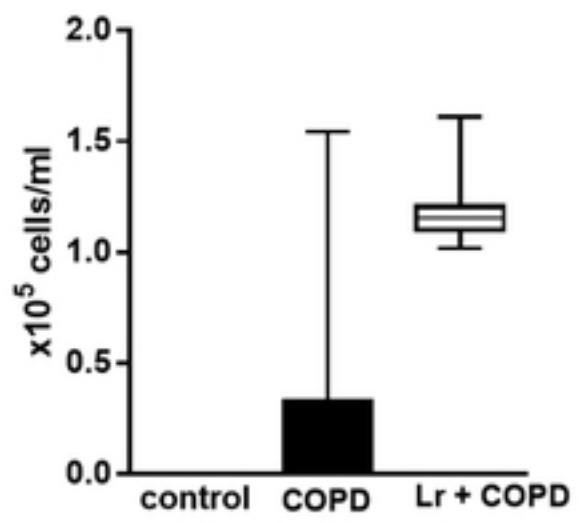


Figure 2

Figure 3

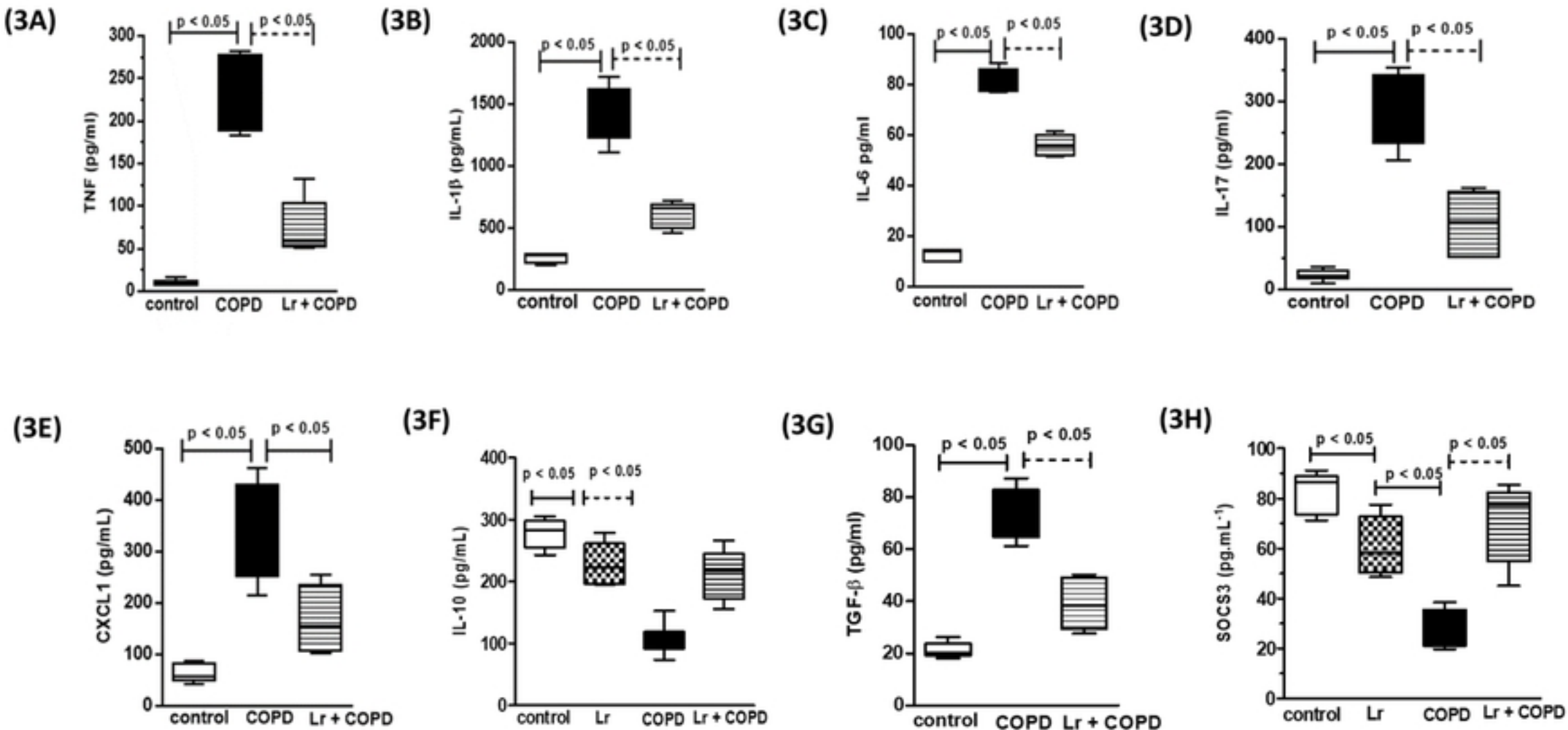


Figure 3

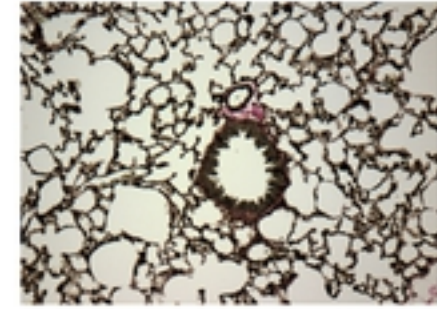
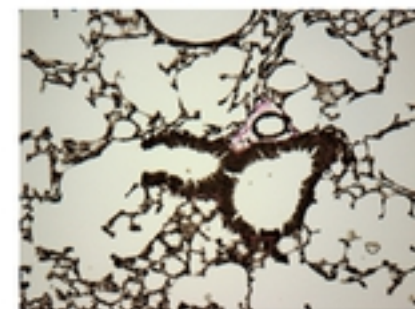
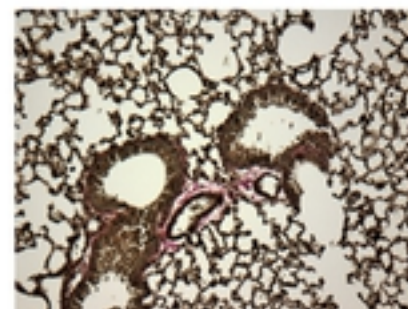
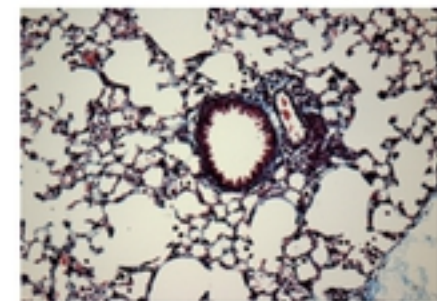
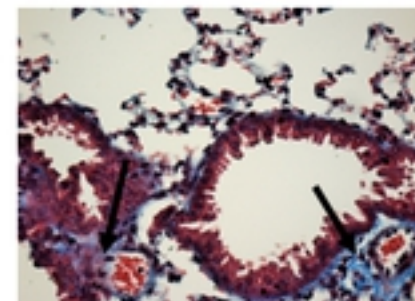
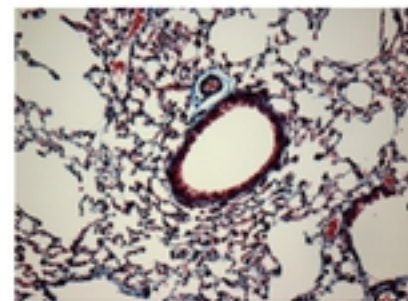
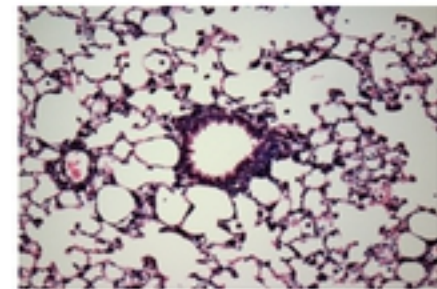
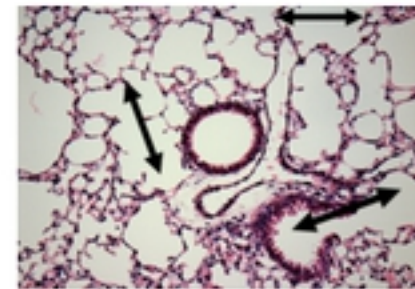
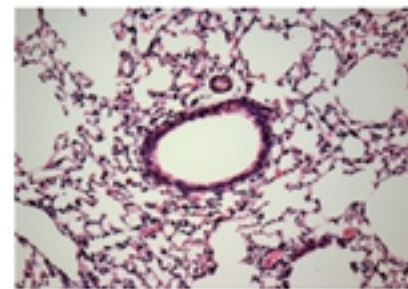
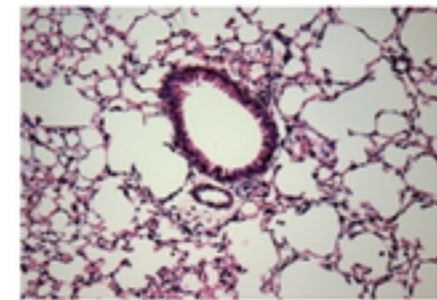
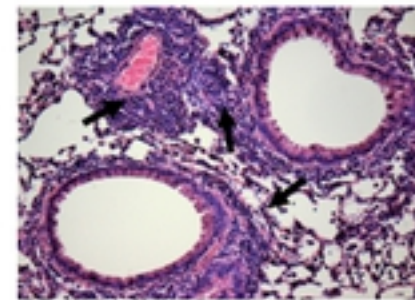
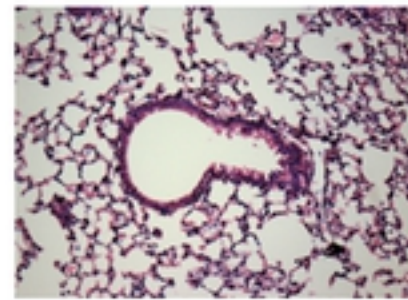
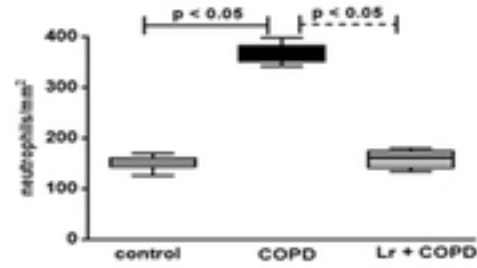
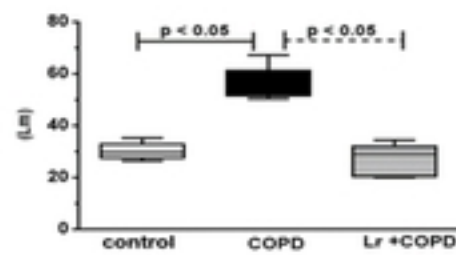
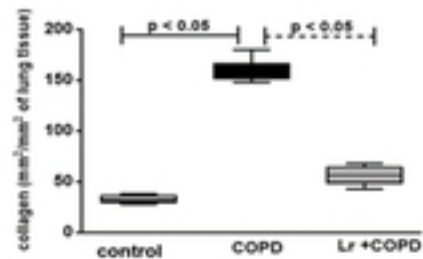
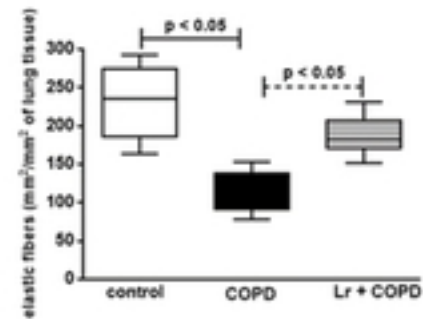
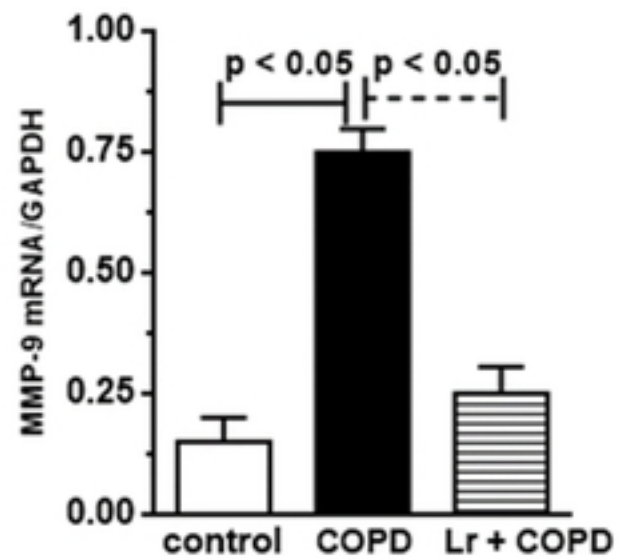
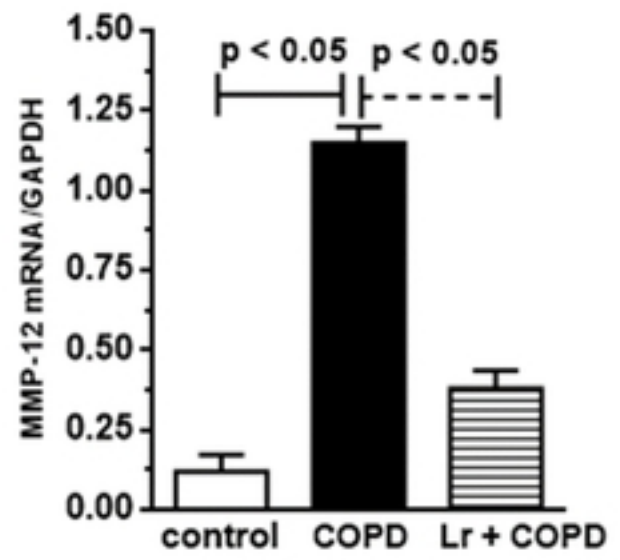
Control**COPD****Lr + DPOC****Figure 4****(4A)****(4B)****(4C)****(4D)****Figure 4**

Figure 5

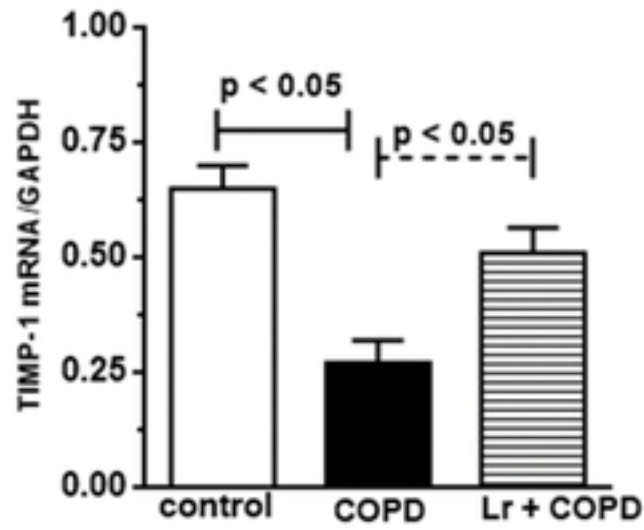
(5A)



(5B)



(5C)



(5D)

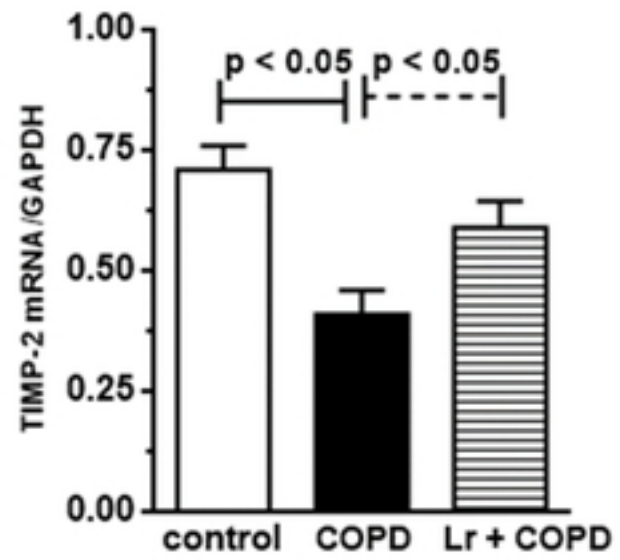


Figure 5

Figure 6

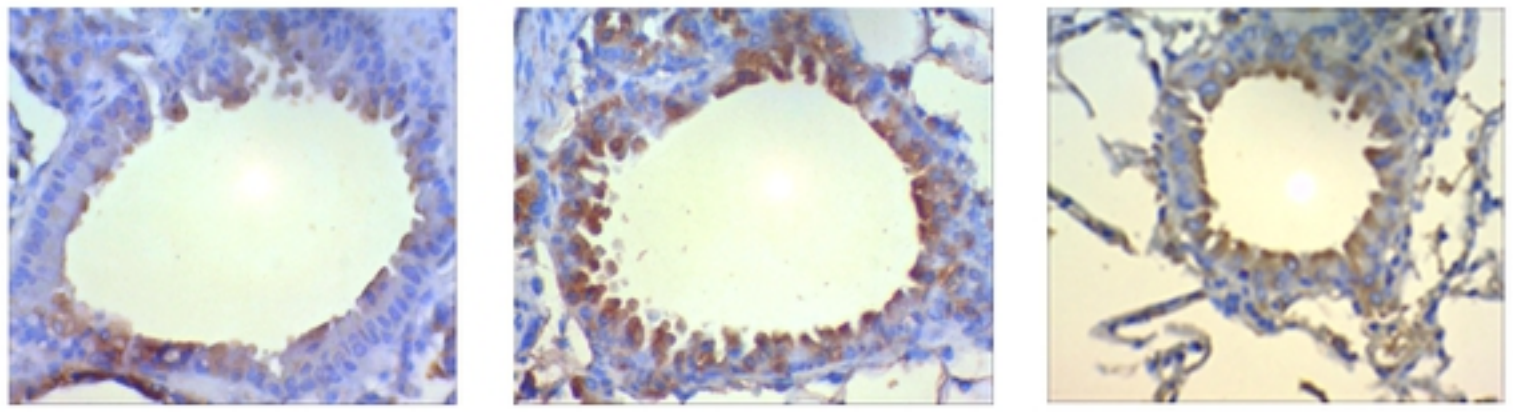
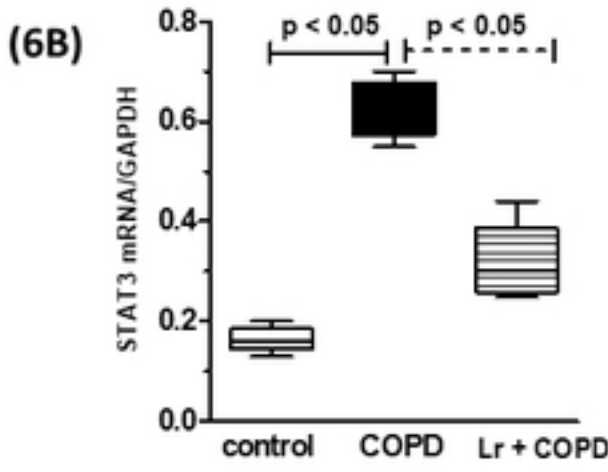
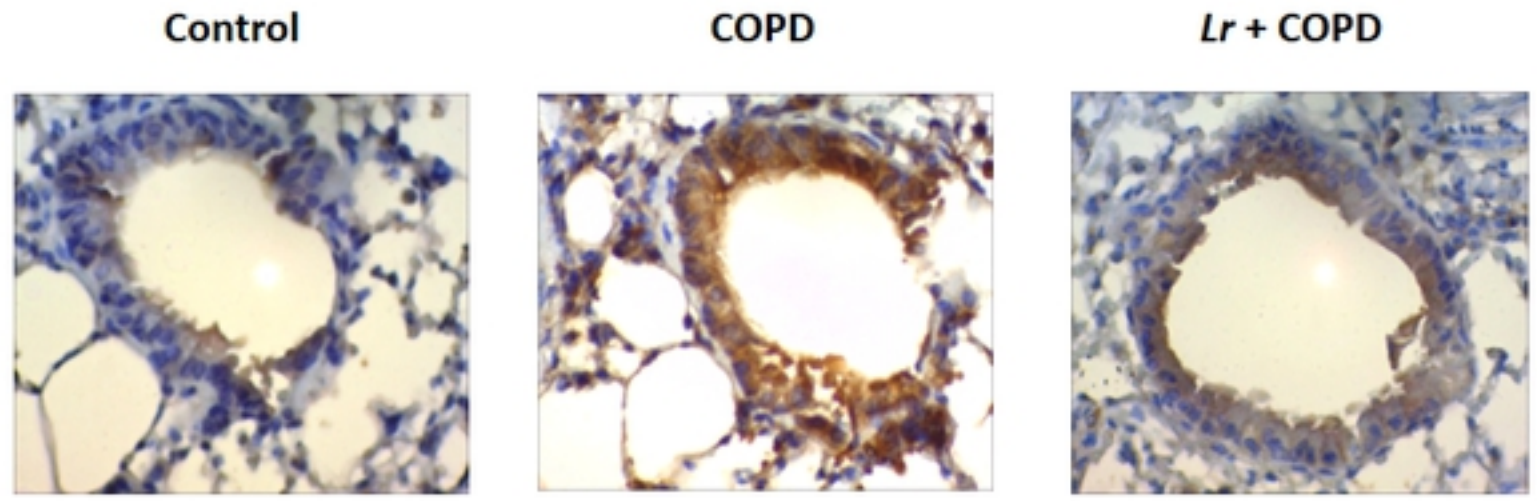
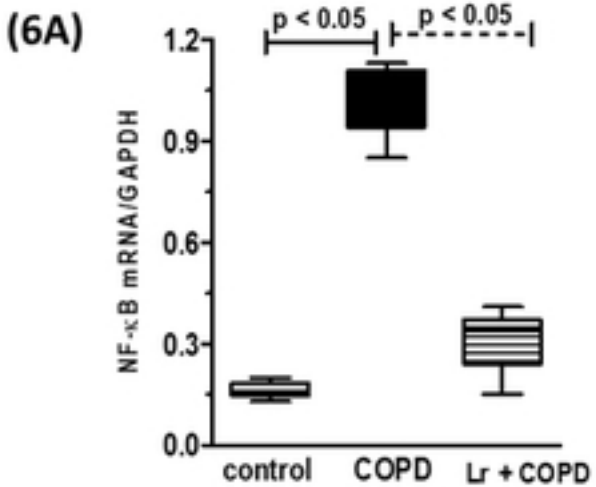


Figure 6

Figure 7

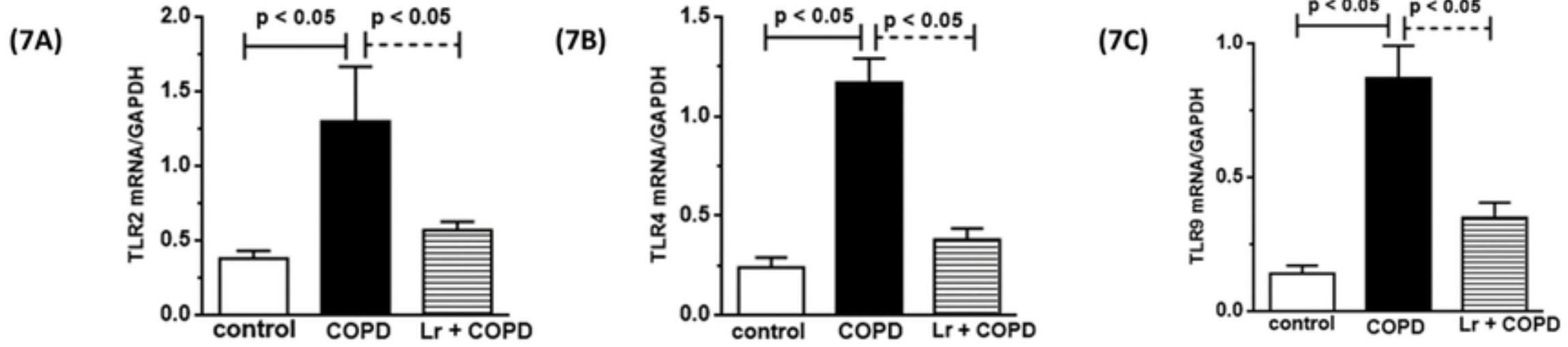


Figure 7

Figure 8

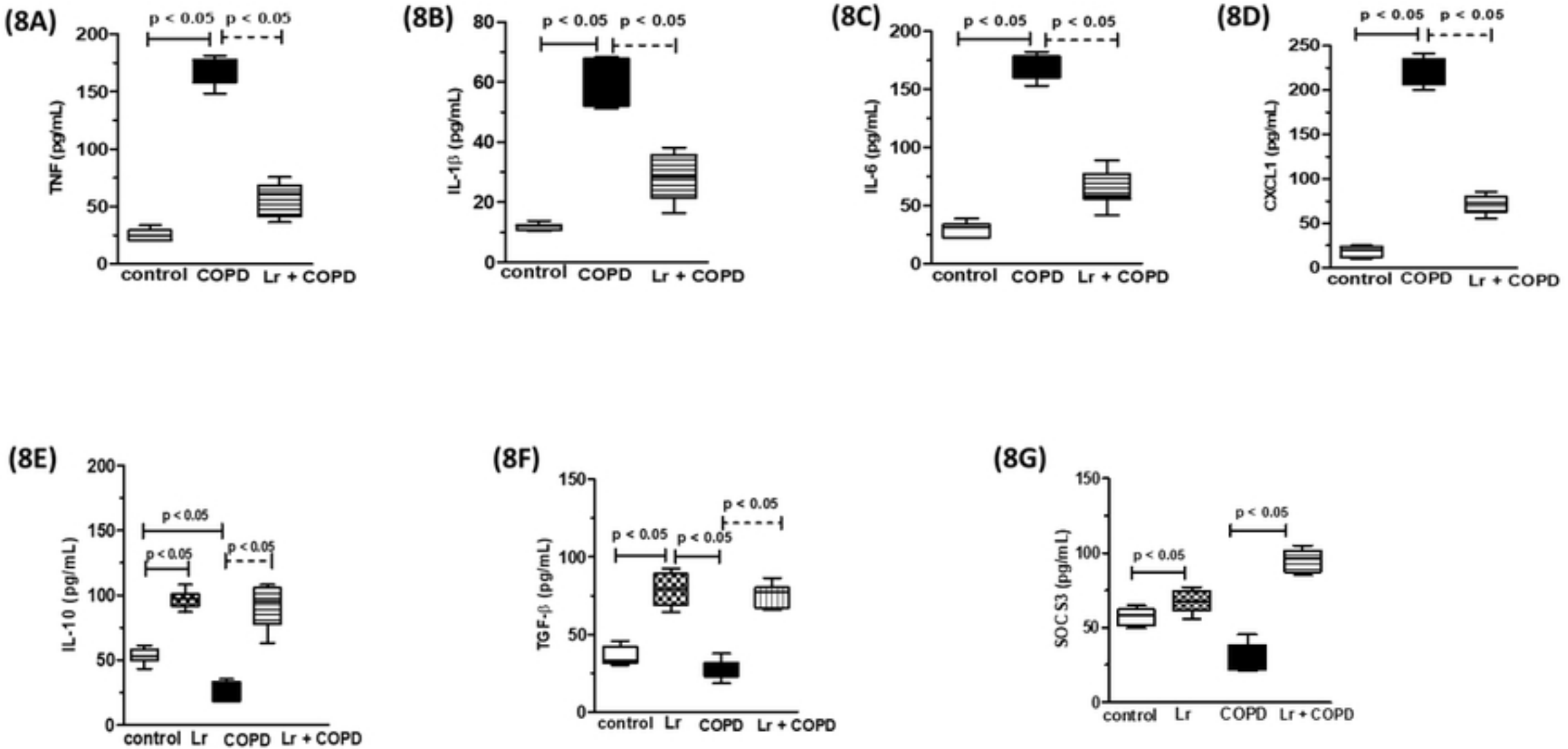


Figure 8

Figure 9

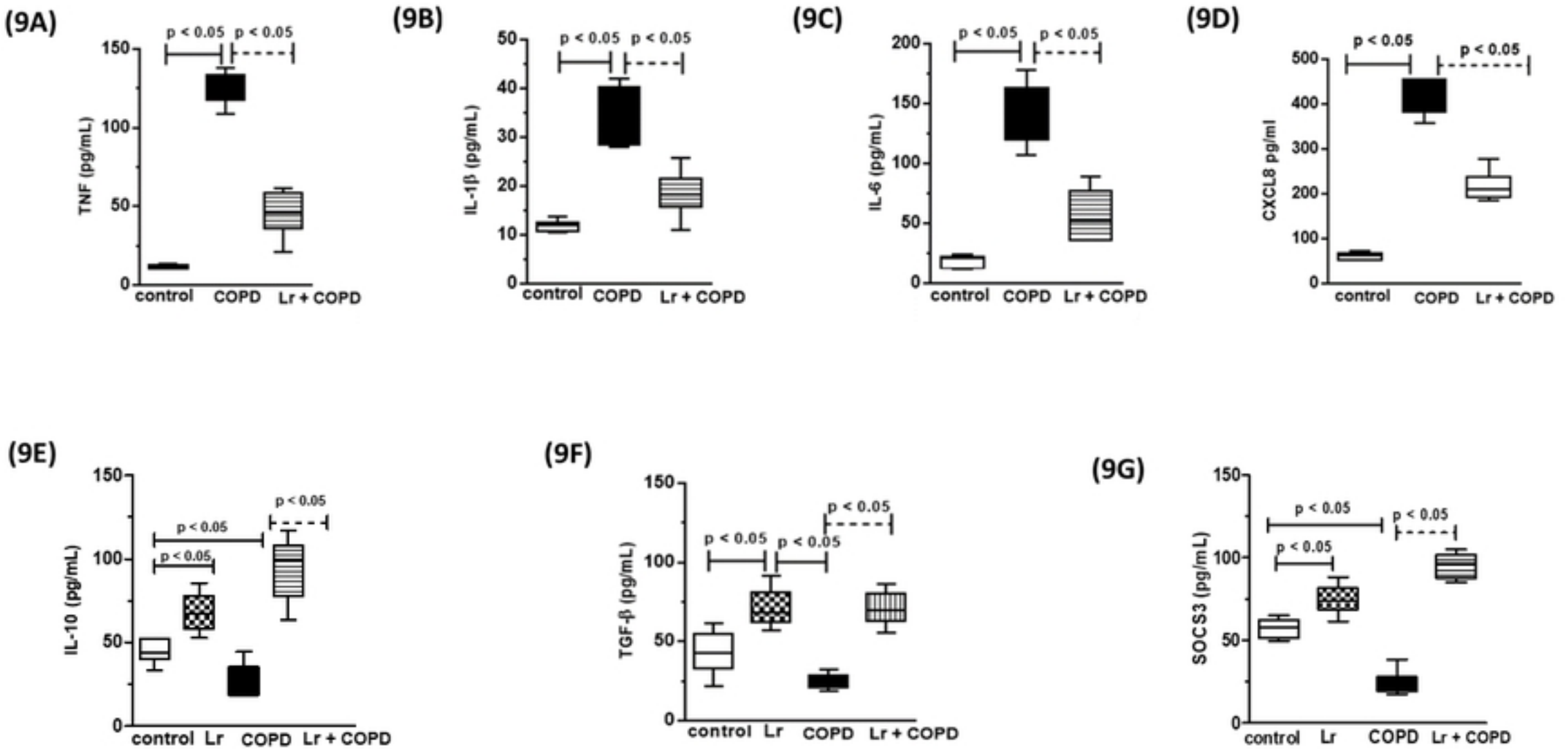


Figure 9

Figure 10

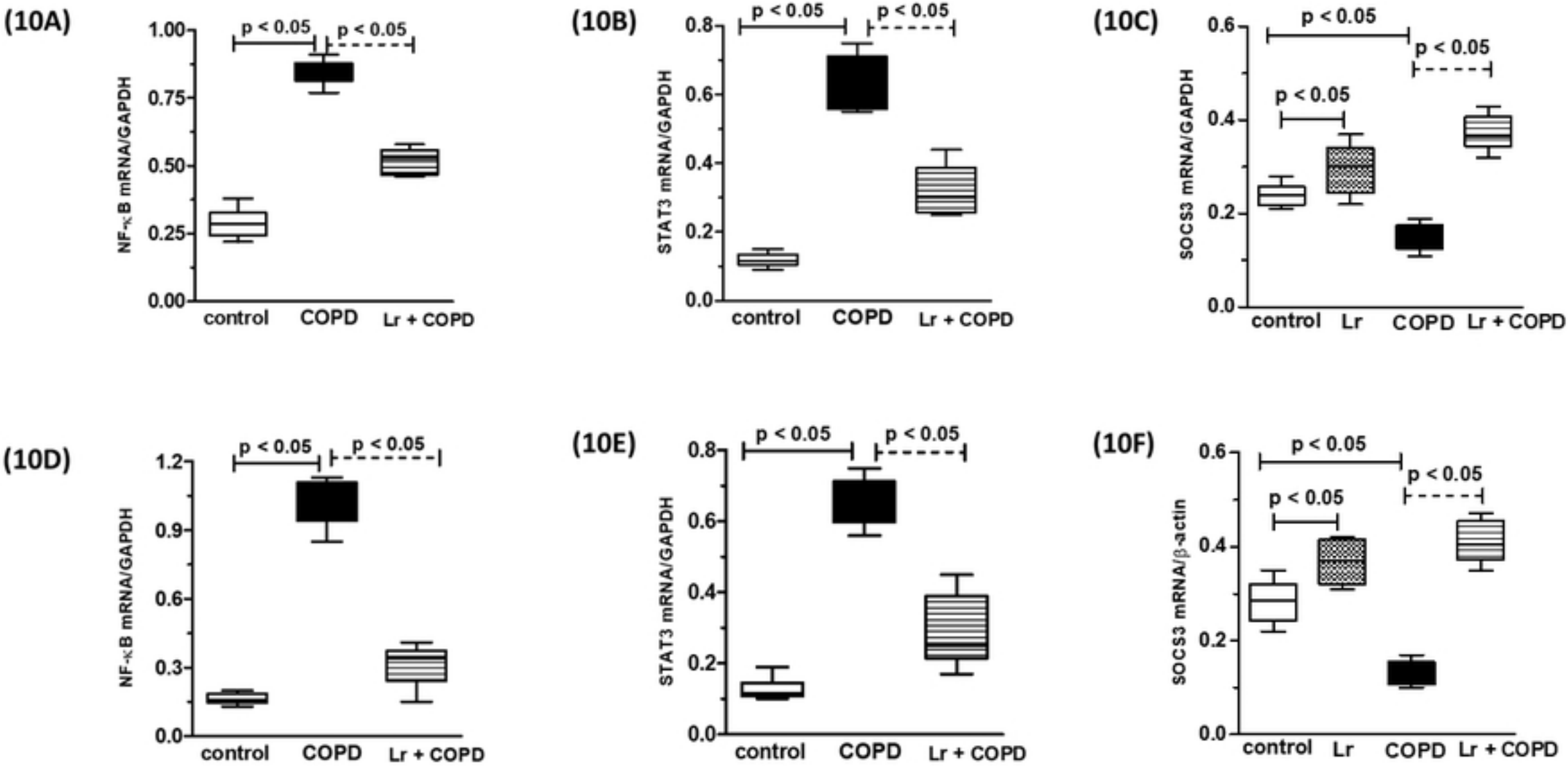


Figure 10

Figure 1

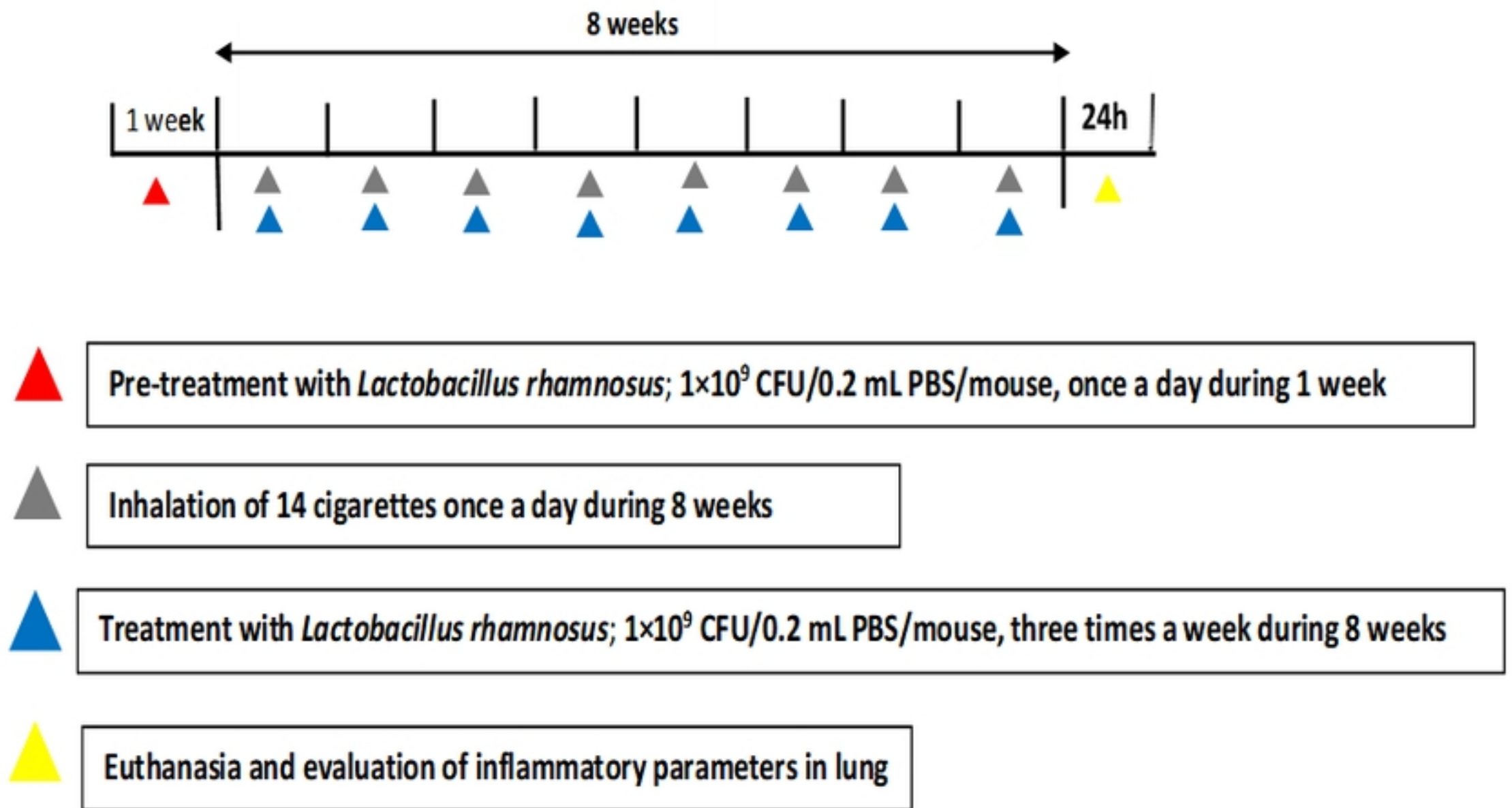


Figure 1